Korean J. Chem. Eng., 40(8), 1970-1985 (2023)
DOI: 10.1007/s11814-023-1477-0

pISSN: 0256-1115
eISSN: 1975-7220

Zirconium-functionalized loofah biocomposite for adsorption catechol and amoxicillin

Junli Wang*, Xu Liu*,†, Huayun Han, and Runping Han*,†**

*College of Chemistry, Zhengzhou University, No 100 of Ke xue Road, Zhengzhou, 450001 P. R. China
**Center for Modern Analysis and Gene Sequencing, Zhengzhou University,
No 100 of Kexue Road, Zhengzhou, 450001 P. R. China
(*Received 12 September 2022 • Revised 5 April 2023 • Accepted 17 April 2023*)

Abstract−Cheap and green loofah as the substrate material was modified with epichlorohydrin and iminodiacetic acid (IDA) to obtain iminodiacetic acid-modified loofah (IDA-LG), and loaded zirconium (IV) onto IDA-LG by a simple complexation reaction to obtain novel biocomposite: zirconium-modified loofah (Zr-IDA-LG). The influence factors and adsorption mechanisms were explored by characterization and adsorption study toward catechol and amoxicillin in batch and fixed-bed modes. The study found that the surface morphology, specific surface area and internal functional groups of the adsorbent changed significantly, the isoelectric point of Zr-IDA-LG was shifted in the acidic direction (2.68 for Zr-IDA-LG) after the modification. This showed that modification of the loofah was successful. The adsorption of catechol and amoxicillin by Zr-IDA-LG showed that the pH range of the material was wide, and the coexisting ions had adverse effects on adsorption. The maximum adsorption capacity of Zr-IDA-LG from Langmuir model was 44.9±11.2 $mg \cdot g^{-1}$ for catechol and 16.8±1.2 $mg \cdot g^{-1}$ for amoxicillin at 293 K. The adsorption isotherm and kinetic model of Zr-IDA-LG manifested that the adsorption process was dominated by monomolecular layer adsorption for catechol and monomolecular layer adsorption for amoxicillin with the presence of heterogeneous adsorption. Both adsorption processes were accompanied by ion exchange. The higher column and lower flow velocity were favorable for the fixed bed adsorption, while the Yan model could fit the fixed bed adsorption behavior. The adsorption quantity in column performance from breakthrough curves was to 20.0 $mg \cdot g^{-1}$ for catechol and 15.8 $mg \cdot g^{-1}$ for amoxicillin. Regeneration with 75% ethanol of spent Zr-IDA-LG was remarkable. The biocomposite is promising for removing some pollutants from water.

Keywords: Modified Loofah, Adsorption, Catechol, Amoxicillin, Regeneration

INTRODUCTION

Phenol compounds are metabolites in the degradation of aromatic pollutants [1]. The source of phenols is the wastewater residue from coking, oil refining, petrochemical, gas power station, pesticide, and other industries [2,3]. The high oxygen consumption of phenolic effluent can break the oxygen balance of water and pose a serious threat to water and aquatic organisms. Phenolic substances can react chemically with human skin and mucous, leading to cellular inactivity. Long-term consumption of phenol-contaminated water can cause dizziness, anemia, and various neurological diseases [4,5]. Catechol is an important chemical intermediate with weak acidity and it is easily oxidized, its dihydroxyl structure can form stable chelates with transition metals [6]. High concentrations of catechol can inhibit the central nervous system of the body, which is highly carcinogenic, teratogenic and mutagenic, directly causing organic lesions in the body [7]. The maximum allowable discharge concentration in our water is 2.0 $mg \cdot L^{-1}$, so how to remove such pollutants from water is one of the popular topics of current research. Amoxicillin, as wide-spectrum antimicrobial, is extensively applied to medicine, animal husbandry, agriculture and other fields. As an emerging organic pollutant, it greatly endangers the ecosystem and human health due to its variety, high content, high toxicity and difficult biodegradation [8]. China is a major country in the use and production of amoxicillin; excessive residues of the medicine in the environment cause the increase of drug resistance of pathogenic bacteria, and the ecological balance is broken [9-11]. Amoxicillin is a kind of β-lactam antibiotic, the structure is more complex than ordinary penicillin antibiotics, and the structure is more stable in an aqueous solution. So it is difficult to degrade and remove through biochemical reactions, which gradually becomes a difficult point of wastewater treatment in the pharmaceutical industry [12]. At present, China has not clearly indicated the maximum allowable discharge concentration in water, so there are few studies on new materials to remove amoxicillin from the environment. The carboxyl group in the molecular structure of amoxicillin can form a stable coordination bond with zirconium, which provides a new idea for its removal [13].

In recent years, the adsorption method has been largely utilized in wastewater treatment due to the cheap economic cost, simple operation, high efficiency and environmental protection [14]. It requires that the adsorbent material must be insoluble in water, the

†To whom correspondence should be addressed.
E-mail: lxcod@zzu.edu.cn, rphan67@zzu.edu.cn

adsorbent has more pores or larger surface area, or the surface contains a structure that can be easily modified by grafting other adsorption functional groups, so that it has the advantages of high efficiency, high speed, high adaptability and easy separation in the removal of pollutants [15]. Compared with other adsorbent materials, biomass is used widely because it is rich in hydroxyl groups, with a wide range of sources and green environmental protection [16,17]. The structure of loofah contains a super active hydroxyl group in each β-D-glucose unit C2, C3 and C6, and the primary hydroxyl group at the C6 position is generally stronger than those at the C2 and C3 [18]. Therefore, not only can loofah use its own hydroxyl functional group for direct adsorption, but also can improve the adsorption effect by loading functional groups through hydroxyl modification of C2, C3 and C6 by etherification and epoxidation [19]. Combined with the three-dimensional pore-like micro-sponge structure of loofah, as well as the physical characteristics of water immersion resistance, corrosion resistance and good mechanical strength and flexibility, it has a wide range of potential applications among the current high-quality biomass adsorption materials [20]. In current research, Ahmad [21] washed, ground, and screened loofah for the removal of Pb^{2+} from aqueous; we found the maximum capacity of Pb^{2+} by native loofah was 24.0 mg·g^{-1} under the optimum conditions of equilibration time of 120 min, pH=6.0, and temperature of 25 °C. The loofah modification treatment is mainly by inorganic acid, alkali soaking, oxidant oxidation, activated carbon activation, and grafting functional groups or polymers to improve the adsorption performance. Kong et al. [22] prepared loofah biochar (LB) and sulfuric acid-treated LB (SLB) from loofah using H_3PO_4 single-step pretreatment and H_3PO_4+H_2SO_4 combined treatment, respectively, and compared the physicochemical properties and removal potential of 4-nitrophenol (4-NP) of those materials. The maximum single-molecule adsorption capacity of 4NP on SLB was 436.6 mg·g^{-1} and 265.4 mg·g^{-1}, respectively. Iminodiacetic acid (IDA) is a semi-EDTA structure, and the adsorption of heavy metal cations can be achieved by using IDA as a modifier [23]. Aryee et al. [24] modified magnetic peanut shells with IDA, which yielded good adsorbent materials. Iminodiacetic acid can also be used as a bridging agent to complex metal ions onto the materials to achieve specific adsorption property toward specific pollutants. Kavakli et al. [25] prepared a chelated fabric with iminodiacetic acid (IDA) as a bridge, loaded with Fe(III), and used to remove phosphate anions. Zirconium is one of the multivalent transition metals, which could effectively improve the selectivity of the adsorbent [26]. Zr(IV) can be complexed with a variety of compounds to form stable empty orbital complexes and also with o-dihydroxy compounds to form stable chelate structures, which are uniquely advantageous for the development of agricultural biomass sorbents for the remediation of polluted water bodies. It also fits the concept of green chemistry [27]. Poude et al. [28] synthesized zirconium-modified garnet peel (SPP@Zr) as a novel biomass-based anion exchanger for the effective remediation of arsenate in polluted water. SPP@Zr showed excellent remediation ability for As(V) with a maximum loading capacity of 83.3 mg·g^{-1} at pH=4.0 and 298 K.

In summary, for effectively changing the pollution status of catechol and amoxicillin, combining the molecular structures of both, IDA was used as a bridge to functionalize loofah, and then zirconium ions with high chelating ability and high coordination ability were used as modifiers to prepare a green and novel zirconium modified adsorbent (Zr-IDA-LG). The results show that the novel adsorbent can effectively remove both contaminants, and thus zirconium-functionalized loofah can be used as a novel non-polluting potential adsorbent material.

EXPERIMENT

1. Experimental Materials

The loofah was soaked in distilled water for 48 h and the water was changed every 12 h. After soaking, the loofah was cleaned with deionized water and dried in a vacuum drying oven at 60 °C. The reagents were analytically pure used in the experiments, and each concentration of catechol and amoxicillin solutions was obtained by diluting 200 mg·L^{-1} stock solution. The main reagents were epichlorohydrin (ECH), iminodiacetic acid (IDA), ethanol (C_2H_5OH), anhydrous sodium carbonate (Na_2CO_3), sodium chloride (NaCl), sodium bicarbonate ($NaHCO_3$), sodium hydroxide (NaOH), anhydrous calcium chloride ($CaCl_2$), catechol ($C_6H_6O_2$), hydrochloric acid (HCl), amoxicillin ($C_{16}H_{25}N_3O_8S$), sodium sulfate (Na_2SO_4), zirconium chloride ($ZrCl_4$).

2. Preparation of Zr-IDA-LG

According to the literature [29], IDA-LG was prepared. Then according to the complexation reaction, 4.0 g IDA-LG was taken in a 500 mL conical flask, 200 mL of 0.3 mol·L^{-1} $ZrCl_4$ aqueous solution (reusable) was added, the pH=3.0 (optimum complexation acidity) of solution was adjusted with 1 mol·L^{-1} NaOH, the solution was vibrated in a water bath at 30 °C for 6 h. Removed and washed with distilled water to neutral, and dried in an oven at 60 °C for 12 h. The zirconium modified loofah (Zr-IDA-LG) was obtained. Fig. 1 shows the preparation flow chart of Zr-IDA-LG.

3. Characterization of Adsorbent

The physical and chemical properties of the adsorbent materials are closely related to adsorption performance and mechanism,

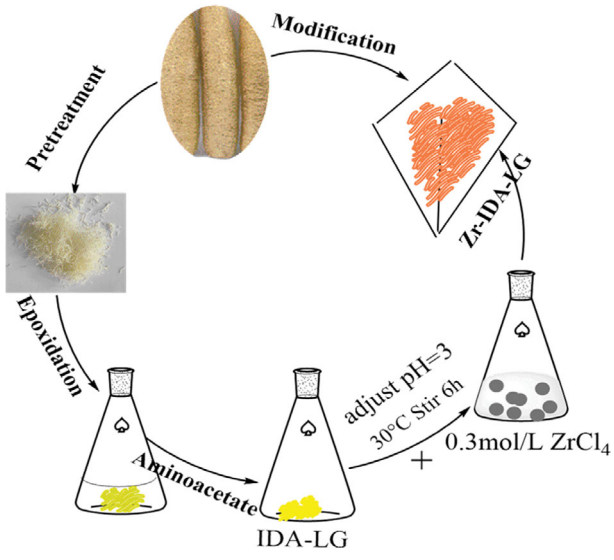

Fig. 1. The synthetic process of Zr-IDA-LG.

so the adsorbent materials' properties need to be characterized [30]. The isoelectric point of the adsorbent was determined by using different pH sodium chloride solutions. The specific surface area of the adsorbent visually indicates the adsorption capacity of the adsorbent, and the material before and after modification was measured according to the nitrogen adsorption and desorption method (BET, ASAP2420, American Mack). Elemental analysis can be used for qualitative and quantitative analysis of organic elements in materials. The C, H, and N contents of the adsorbed materials before and after modification were determined by elemental analysis (Flash EA 1112, USA). X-ray photoelectron spectroscopy (XPS, Escalab 250Xi, Thermo Fisher Scientific) can be used to qualitatively and quantitatively analyze the elemental composition and content of the material surface, as well as analyze the chemical valence state of the elements, chemical bonding and other information and infer the adsorption mechanism. Scanning electron microscopy (SEM, Su8020, China Tianmei Scientific Instruments Co., Ltd.) was used to characterize the microscopic morphology of the material. Fourier transform infrared spectroscopy (FTIR, PE-1710FTIR, American PE company) was used to determine the functional groups contained inside the material before and after modification.

4. Batch and Fixed-bed Adsorption Research

4-1. Batch Adsorption Experiment

Batch and column adsorption provides a theoretical basis for the practical treatment of industrial wastewater. The effects of a series of external environments on batch and fixed bed adsorption processes are performed [31]. The influence factors of batch adsorption mainly include pH, temperature, time, coexisting ion concentration and so on. The specific practice of batch adsorption was to take 10 mg adsorbent into a 50 mL conical flask, add 10 mL adsorbate to it, seal the conical flask and put it into a constant temperature shaker and stir at a constant speed of 120 rpm, and take out the filter after reaching the adsorption equilibrium, then measure the remaining catechol (λ=275.0 nm) and amoxicillin (λ=272.0 nm) by UV spectrophotometer. The unit adsorption amount q_e was obtained by Eq. (1).

$$q = \frac{V(C_0 - C)}{m} \tag{1}$$

where q is the unit adsorption quantity ($mg \cdot g^{-1}$), m is the dosage of adsorbent (g), V is the volume of adsorbate solution (L), C_0 and C are the density of adsorbate before and after adsorption ($mg \cdot L^{-1}$), respectively.

4-2. Column Adsorption Experiment

The method of column adsorption was to load a certain mass of adsorbent into a acid burette with length 40 cm and inner diameter 1.0 cm. The bottom was compacted with cotton to prevent the adsorbent from leaking out of the bottom of the column, and the top was stuffed with cotton to prevent the adsorbent material from floating. Column uptake experiment was performed at 293 K and pH 6. The experiments were performed by pumping catechol and amoxicillin solution into the column in downward flowing mode with one peristaltic pump and the effluent was taken at regular intervals in the process. Various concentrations (13, 30, 45 $mg \cdot g^{-1}$), flow rates (4, 6, 8 $mL \cdot min^{-1}$), bed heights (2.0, 3.5, 5.0 cm for catechol, 2.0, 4.0, 6.0 cm for amoxicillin) were designed to study the effect on breakthrough curves. The concentration of the effluent was measured in a specified time, plot the penetration curve with C_t/C_0 about time. The total adsorption quantity q_{tatal} ($mg \cdot g^{-1}$) and unit adsorption quantity q_{exp} ($mg \cdot g^{-1}$) for fixed bed adsorption were obtained using Eq. (2) and (3). The mass of total adsorbed mass W_{total} and the removal efficiency (Y) could be calculated by Eq. (4) and (5).

$$q_{total} = \frac{v}{1000} \int_{t=0}^{t=t_{total}} (C_0 - C_t) dt \tag{2}$$

$$q_{exp} = q_{total}/m \tag{3}$$

$$W_{total} = \frac{vC_0 t_{total}}{1000} \tag{4}$$

$$Y = \frac{q_{total}}{W_{total}} \times 100\% \tag{5}$$

where C_0 ie the initial adsorbate concentration while C_t is the concentration of effluent at time t ($mg \cdot L^{-1}$), v is the flow rate ($mL \cdot min^{-1}$), m is the mass of modified loofah in column.

5. Desorption and Regeneration

5-1. Batch Desorption and Regeneration

To fully reflect the principles of green chemistry, desorption and regeneration experiments of catechol or amoxicillin loaded Zr-IDA-LG were carried out. The desorption solutions are water, ethanol, sodium hydroxide, hydrochloric acid and sodium sulfate. The desorption rate d and regeneration rate r are calculated by the following equations.

$$d = \frac{m_d}{m_0} \times 100\% \tag{6}$$

$$r = \frac{q_r}{q_m} \times 100\% \tag{7}$$

where m_d is the mass (mg) of adsorbate desorbed during desorption, and m_0 is the mass (mg) of adsorbate on adsorbent before desorption.

5-2. Fixed Bed Desorption and Regeneration

We selected the desorption solution with the best effect in the batch desorption regeneration experiment for column desorption regeneration, and the concentration of adsorbate in the effluent C_t ($mg \cdot g^{-1}$) was measured at different times (min) until the concentration of the effluent reached the minimum and remained basically unchanged. The desorption rate and regeneration rate were calculated by repeating the desorption experiment twice under the same experimental conditions, the adsorbate mass m_d from could be obtained from Eq. (8)

$$m_d = \frac{v}{1000} \int_{t=0}^{t=t_{total}} C_t dt \tag{8}$$

6. Error Analysis

The experimental data were the average of three experiments with an error of less than 5%, all those were represented by vertical error bars. In the process of nonlinear fitting for the experimental data, for judging whether the model can be used to describe the adsorption process, the determined coefficient (R^2) and the sum of squared errors (SSE) are generally chosen as the basis. SSE has

an extremely important value in the practical application process.

$$SSE = \sum (q_c - q_e)^2 \quad (9)$$

where q_c and q are values of the adsorption quantity from models and experiments.

RESULTS AND DISCUSSION

1. Characterization of Materials

(1) BET: From the instrumental data, we could obtain that the specific surface area of the modified materials all increased, the specific surface area of IDA-LG was 1.57 $m^2 \cdot g^{-1}$, which may be that after the original loofah was treated with NaOH, some lignin on the surface was dissolved, thus expanding the specific surface area of the material. While the specific surface area of Zr-IDA-LG decreased from 1.57 $m^2 \cdot g^{-1}$ to 0.019 $m^2 \cdot g^{-1}$, probably because the zirconium loaded on the surface of loofah blocked some pore structures, resulting in the reduction of the specific surface area [32]. Combined with the SEM analysis, in Fig. 2(a), it can be seen that the surface of the loofah before modification had obvious microporous structure, but it was not detected in the test. The reason may be the specific surface area of LG was lower than detection limit of the instrument, leading to a result of 0 $m^2 \cdot g^{-1}$.

(2) EA: Iminodiacetic acid contains an amino group, so it can be proved whether the modification is successful by the change of nitrogen content in the modified material. Elemental analysis of the three adsorbent materials was performed, and the results are shown in Table 1. According to data in Table 1, there was no nitrogen in the original loofah. The nitrogen content of IDA-LG and Zr-IDA-LG increased from 0 to 0.315% and 0.405%. The above experimental data indicated that IDA was successfully introduced to loofah.

Table 1. Elemental analysis results of loofah before and after modification

Sample	N %	C %	H %
LG	-	44.9	5.93
IDA-LG	0.315	43.9	6.25
Zr-IDA-LG	0.405	44.5	6.09

(3) SEM: Fig. 2(a) and 2(b) shows the SEM images of LG and IDA-LG. The native loofah is smoother and the structure is neatly arranged [33]. From Fig. 2(a) and 2(b), it can be seen that the surface of the modified adsorbent is uneven and the specific surface area is expanded. Fig. 2(c) shows the SEM images of Zr-IDA-LG; the surface became rough and uneven, with more obvious crystalline and granular impurity particles, and the particles of different sizes were disorderly embedded in the uneven distribution, indi-

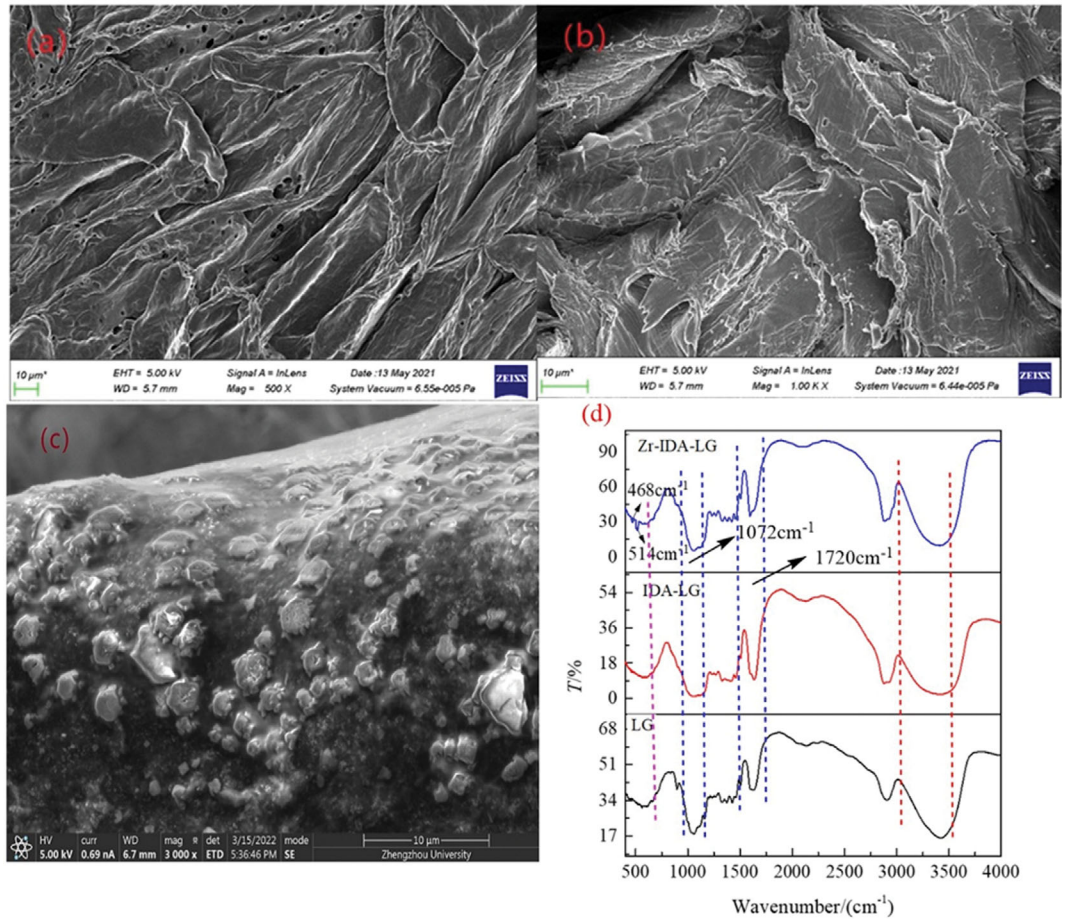

Fig. 2. Scanning electron microscopy and FTIR diagram ((a) LG; (b) IDA-LG; (c) Zr-IDA-LG; (d) FIRT).

cating that the modified IDA-LG had formed a new complex with Zr^{4+}, thus the material was successfully modified.

(4) FTIR: Fig. 2(d) shows the infrared spectra before and after modification. The peaks broaden of the modified material at the wave number 3,000-3,500 cm^{-1}, and the modified peaks become strong and sharp at the wave number 1,720 cm^{-1}, which is due to introduce more carboxyl groups in the material. The peaks of the modified material broaden at 1,072 cm^{-1}, which is the stretching vibration peak of -C-N, besides the contribution of C-O stretching vibration [34]. In the FTIR of Zr-IDA-LG, the peaks of the stretching vibration of Zr-O appear at the wavelengths of 468 cm^{-1} and 514 cm^{-1}, which proves that zirconium exists on surface of IDA-LG.

2. Batch Adsorption Study

2-1. Isoelectric Point Analysis and Effect of pH

At pH below the isoelectric point of the adsorbent, a positive charge appears on the surface of the material. Otherwise, it is negatively charged. The results are shown in Fig. 3(a). The isoelectric point is 6.50, 5.12, 2.68 for LG, IDA-LG and Zr-IDA-LG, respectively. The reason is mainly due to pH<1 of zirconium chloride solution (H_2O, 20 °C). It was strongly acidic, according to the Lewis acid-base theory, the empty orbital from zirconium could accept the lone pair electrons in the solution, thus moving the isoelectric point towards the acid [35].

Fig. 3(b) shows the influence of pH on the adsorption of catechol by Zr-IDA-LG, when the pH=2.0-6.0, the q_e increased from 13.5 $mg \cdot g^{-1}$ to 18.1 $mg \cdot g^{-1}$. When the pH=6.0-8.0, the q_e tends to be stable, and when the pH=8.0-11.0, the q_e decreases significantly. Combined with the isoelectric point analysis, the pH_{pzc} of Zr-IDA-LG is 2.68, material surface is negatively charged, and the adsorption is easy to carry out in the acidic environment. When the pH>8, the negative charge in the solution generates electrostatic repulsion with the material surface, which significantly reduces the adsorption capacity, indicating that there exists electrostatic attraction in the adsorption process [36]. The pK_{a1}=9.45 and pK_{a2}=12.8 of catechol, then in the range of pH=2.0-9.45, catechol exists in molecular form, so there is complexation during adsorption. The influence of solution pH on the amoxicillin adsorption is presented in Fig. 3(c). In the range of pH=2-10, according to the molecular struc-

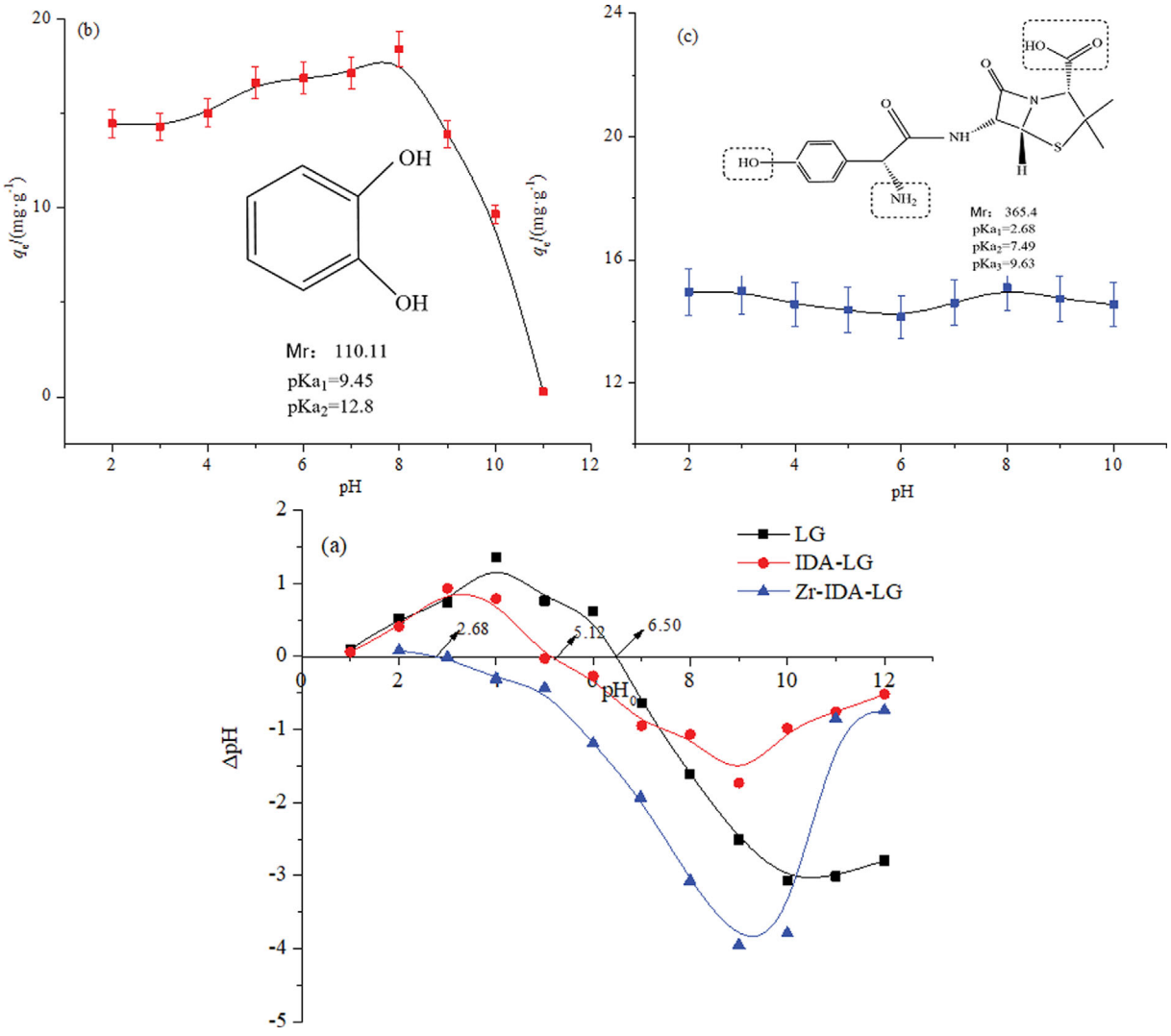

Fig. 3. Isoelectric point diagram (a); effects of pH on catechol (b) and amoxicillin (c).

ture of amoxicillin, it possesses a large number of amino, carboxyl and phenolic hydroxyl groups. Under the different pH conditions, these functional groups produce different ionization reactions. When the pH<2.68, the groups in the amoxicillin molecule could be protonated. When the pH=2.68-7.49, the amoxicillin molecule is close to neutral, because of the carboxyl groups begins to ionize, while the protonation degree gradually decreases. When the pH>7.49, the phenolic hydroxyl group is ionized, the amoxicillin molecule is present as an anion in the water. Combined with isoelectric point analysis, when the pH>2.68, the surface of the material is negatively charged, the adsorbate exists mainly of neutral molecules and anions. With the increasing of pH, the q_e remains basically unchanged. It is speculated that amoxicillin may have a macromolecular structure. Although there is electrostatic repulsion, there is still a chemical adsorption (such as complexation) in the process, which is dominated by chemical adsorption. Therefore, it proves that the modified material has a wider pH range for the adsorption of amoxicillin.

2-2. Effect of Coexisting Ions

The presence of coexisting ions dilutes the concentration of adsorbate molecules and the total number of ions in solution, thus affecting the adsorption process and mechanism. Therefore, it is important to study the effect of coexisting ions on adsorption. In Fig. 4(a), the q_e of catechol by Zr-IDA-LG decreases from 19.4 $mg \cdot g^{-1}$ to 13.2 $mg \cdot g^{-1}$, 10.1 $mg \cdot g^{-1}$, 4.91 $mg \cdot g^{-1}$ with the increase of ion concentration. As the effect of SO_4^{2-} is greater than Cl^-, it could be speculated that the adsorption is accompanied by ion exchange or electrostatic attraction. The effect of HCO_3^- was the greatest on the adsorption, probably due to the hydrolysis of HCO_3^- to produce OH^-, which changes the pH of the solution and causes the OH^- onto the surface of the material, thereby significantly reducing the adsorption capacity. This is consistent with the conclusion from effect of pH on adsorption. As shown in Fig. 4(b), in the adsorption of amoxicillin by Zr-IDA-LG, the q_e shows a downward trend with the increasing of ion concentration, and the q_e decreases from 15.4 $mg \cdot g^{-1}$ to 12.5 $mg \cdot g^{-1}$, 10.3 $mg \cdot g^{-1}$, so it could be considered that there is ion exchange, electrostatic attraction, etc. However, in the presence of higher ions concentrations, the adsorbent still has the ability for pollutants, indicating that there are other forces in the adsorption process [37].

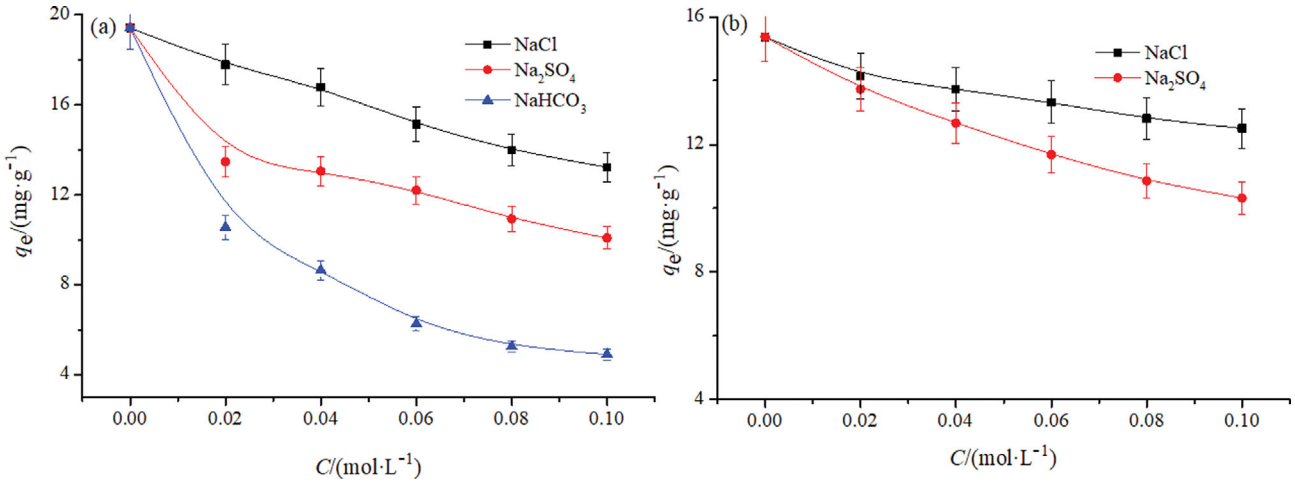

Fig. 4. Effects of co-existing ion on catechol (a) and amoxicillin (b).

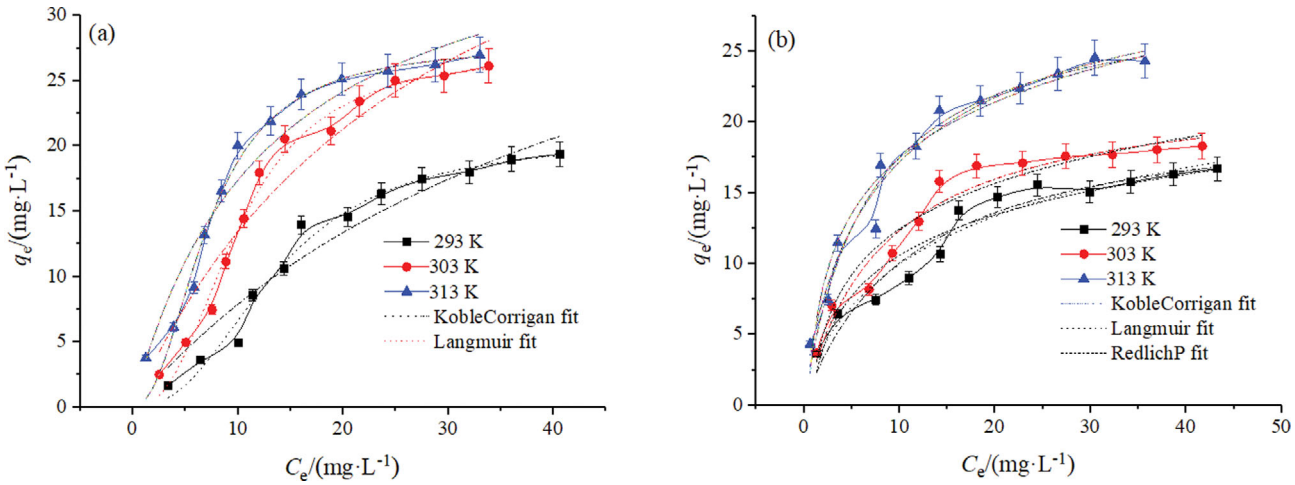

Fig. 5. Effects of catechol (a) and amoxicillin (b) concentration on adsorption and fitted isotherm curves.

2-3. Adsorption Isotherm Model Fitting Analysis

The equilibrium adsorption data were modeled by adsorption isotherms to explore the adsorption mechanism, surface properties of the adsorbent and the maximum adsorption capacity, which provide some theoretical basis for the practical application for adsorbent [38]. In Fig. 5, when the concentration of catechol and amoxicillin is small, there exist abundant adsorption sites on Zr-IDA-LG. When the concentration increases, a large number of adsorption sites on Zr-IDA-LG are occupied, so the adsorption gradually reaches saturation and the adsorption amount basically no longer increases. With the increase of temperature, the q_e of the same concentration also increases; thus it was proved that the adsorption of catechol and amoxicillin by Zr-IDA-LG was an endothermic process. Taking catechol as an example, when the initial concentration of catechol was 30.0 $mg \cdot g^{-1}$, and the adsorption equilibrium was reached, the q_e of catechol at 293 K, 303 K and 313 K were 13.9 $mg \cdot g^{-1}$, 17.9 $mg \cdot g^{-1}$ and 20.0 $mg \cdot g^{-1}$, respectively.

Three isotherm models are used to fit the experimental data of

Table 2. The adsorption model used in the text

	Model name	Nonlinear equations	Model meaning
Isothermal adsorption model	Langmuir	$q_e = \frac{q_m K_L C_e}{1 + K_L C_e}$	Used to describe whether the reaction is a homogeneous monolayer adsorption process
	Redlich-Peterson	$q_e = \frac{AC_e}{1 + BC_e^g}$	The adsorption mechanism is a hybrid adsorption
	Koble-Corrigan	$q_e = \frac{AC_e^n}{1 + BC_e^n}$	When n is close to 1, the model is close to Langmuir model; when 0<n<1, the model is close to Freundlich
Kinetic adsorption model	Elovich equation	$q_t = \frac{\ln(a\beta)}{\beta} + \frac{\ln t}{\beta}$	It is a description of heterogeneous diffusion determined by reaction speed and diffusion coefficient.
	Double constant equation	$\ln q_t = \ln A + K_s t$	This model only expresses the initial stage of adsorption, but cannot describe the whole process of adsorption accurately.
Column adsorption model	Yan	$\frac{C_t}{C_0} = 1 - \frac{1}{1 + (vt/b)^a}$	This model expresses the initial stage of penetration curve, the error caused by using Thomas model is reduced.

Table 3. Isotherm fitting results of adsorption of Zr-IDA-LG toward catechol and amoxicillin

Langmuir						
	T/(K)	$K_L/(L \cdot mg^{-1})$	$q_{e(exp)}/(mg \cdot g^{-1})$	$q_{m(theo)}/(mg \cdot g^{-1})$	R^2	SSE×10^2
Catechol	293	2.11±0.82	19.3	44.9±11.2	0.932	26.8
	303	3.46±1.13	25.3	52.0±9.9	0.932	48.0
	313	7.74±1.74	27.0	39.7±3.9	0.941	40.8
Amoxicillin	293	5.42±2.31	17.0	16.8±1.2	0.611	0.036
	303	0.701±0.145	20.7	20.7±0.8	0.901	0.017
	313	1.15±0.23	21.3	21.0±0.8	0.884	0.022
Redlich-Peterson						
	T/(K)	K	A	g	R^2	SSE
Amoxicillin	293	3.02±1.89	0.315±0.423	0.807±0.178	0.935	11.7
	303	2.06±0.49	0.0429±0.0456	1.19±0.22	0.949	11.8
	313	5.29±1.84	0.258±0.213	0.905±0.130	0.964	15.4
Koble-Corrigan						
	T/(K)	A	B	n	R^2	SSE×10^2
Catechol	293	3.51±3.26	0.171±0.151	2.44±0.38	0.978	8.02
	303	8.62±6.10	0.317±0.216	2.49±0.32	0.983	10.9
	313	35.2±21.7	1.27±0.75	2.22±0.32	0.976	14.7
Amoxicillin	293	2.81±0.91	0.104±0.027	0.746±0.22	0.940	10.8
	303	2.79±0.97	0.122±0.033	0.975±0.223	0.946	12.5
	313	5.31±1.10	15.9±2.7	0.822±0.171	0.966	14.5

Zr-IDA-LG for the adsorption of catechol and amoxicillin. The model expressions are shown in Table 2, and the fitting curves are also shown in Fig. 5 and parameters of models are listed in Table 3. In the fitting of experimental data for the adsorption of catechol, the R^2 of the Koble-Corrigan model was greater than 0.976 and the SSE value was smaller. Furthermore, the fitted curves from this model were closer to the experimental curves. So it could be used to describe the adsorption equilibrium behavior. The fitting data n>1 in the Koble-Corrigan model, it was biased towards the Langmuir model, which was dominated by monomolecular layers.

In the fitting of experimental data for adsorption of amoxicillin, the Langmuir model R^2 was greater than 0.9, the theoretical adsorption capacity was not much different from the actual adsorption capacity, so it could be used to describe the adsorption process. For the Redlich-Peterson model, there were higher values of R^2 (>0.973) and smaller values of SSE; this shows that this model could be used to describe the adsorption process, indicating that there was hybrid adsorption rather than ideal monolayer. For the Koble-Corrigan model, as there were also higher values of R^2 (>0.94), and the values of n were between 0 and 1, the model was more in

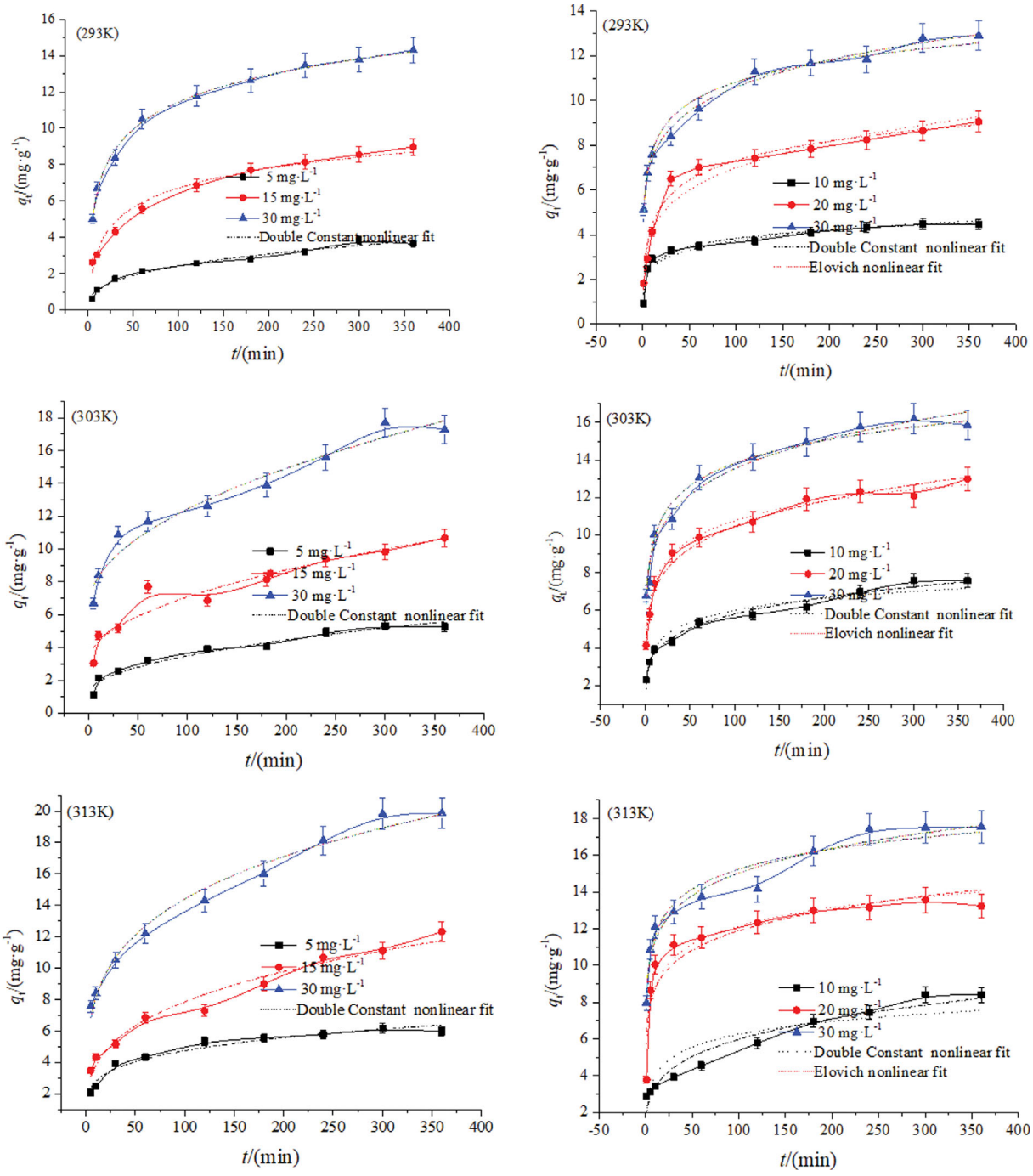

Fig. 6. Effects of time at different temperatures and fitting kinetic curve about catechol (left) and amoxicillin (right).

line with the Freundlich model. In summary, the adsorption process was a multiphase non-ideal single-molecular adsorption.

2-4. Adsorption Kinetics Model Fitting Analysis

The kinetic study of the adsorption reaction is usually used to describe the rate of adsorption and the results are depicted in Fig. 6. It is obviously found that the adsorption of catechol and amoxicillin by Zr-IDA-LG is divided into fast adsorption, medium adsorption and slow adsorption. With the increase of time, the adsorption capacity first increases, then decreases and finally tends to equilibrium. At the three different initial concentrations (5 $mg \cdot L^{-1}$, 15 $mg \cdot L^{-1}$, 30 $mg \cdot L^{-1}$), a large amount of adsorbate migrates to the Zr-IDA-LG surface with increasing initial concentration, directly contributing to the equilibrium adsorption amount increasing, and the time required to reach equilibrium also increasing [39]. At the three temperatures, the adsorption capacity increases by the increase of temperature, which proves that it is an endothermic reaction. As the temperature increases, the molecular mobility of the adsorbent (kinetic effect) and the number of active sites in the adsorption process on the surface of the adsorbent increases, resulting in an increase of adsorption capacity of the same concentration [40]. Taking catechol at a concentration of 30 $mg \cdot L^{-1}$ as an example, the q_e for reaching adsorption saturation were 14.3 $mg \cdot g^{-1}$, 17.3 $mg \cdot g^{-1}$, and 19.9 $mg \cdot g^{-1}$ at three temperatures. Vunain [41] used sunflower seed husk residue biochar as adsorbent to adsorb ortho-diphenol and resorcinol from aqueous, and the results were similar and consistent with the kinetic results. In this paper, two adsorption kinetic models were used to fit the experimental data for the adsorption of catechol and amoxicillin; the model expressions are shown in Table 2, and the fitting results are in Fig. 6 and Table 4. The Double Constant equation model had a large value of R^2 (>0.92) and a small value of SSE in the adsorption of catechol while the fitting curves were closer to experimental points. Therefore, we used it to describe the adsorption behavior, indicating that there was heterogeneous diffusion in the adsorption process, which was consistent with the results of adsorption isotherm studies. In the adsorption reaction of amoxicillin, both Elovich equation (R^2>0.91) and Double

Table 4. Kinetic fitting results of adsorption of Zr-IDA-LG toward catechol and amoxicillin

Double constant equation						
	T/K	$C_0/(mg \cdot L^{-1})$	A	ks	R^2	SSE
Catechol	293	10	0.486±0.070	0.349±0.027	0.973	0.232
		20	1.66±0.08	0.290±0.009	0.995	0.211
		30	3.98±0.23	0.221±0.012	0.985	1.20
	303	10	0.911±0.114	0.303±0.024	0.970	0.461
		20	2.34±0.36	0.251±0.029	0.928	3.30
		30	4.91±0.44	0.213±0.018	0.961	3.97
	313	10	1.64±0.17	0.231±0.020	0.960	0.646
		20	1.85±0.24	0.314±0.025	0.968	2.23
		30	4.57±0.33	0.249±0.014	0.982	0.363
Amoxicillin	293	10	1.71±0.19	0.170±0.023	0.902	0.962
		20	2.54±0.31	0.220±0.024	0.939	3.08
		30	5.16±0.15	0.157±0.006	0.991	0.530
	303	10	2.29±0.13	0.202±0.011	0.982	0.482
		20	4.70±0.24	0.174±0.010	0.978	1.59
		30	6.57±0.31	0.157±0.009	0.975	2.45
	313	10	1.91±0.26	0.248±0.026	0.936	2.45
		20	6.41±0.70	0.134±0.022	0.937	2.08
		30	8.51±0.39	0.124±0.001	0.959	3.34
Elovich equation						
	T/K	$C_0/(mg \cdot L^{-1})$	$\alpha/(g \cdot mg^{-1} \cdot min^{-1})$	$\beta/(g \cdot mg^{-1}) \times 10^2$	R^2	SSE
Amoxicillin	293	10	1.32±0.17	0.547±0.039	0.955	0.439
		20	1.53±0.29	1.27±0.07	0.975	1.29
		30	4.59±0.33	1.36±0.08	0.972	1.64
	303	10	1.84±0.31	0.906±0.072	0.946	1.45
		20	3.84±0.23	1.51±0.05	0.989	0.817
		30	5.78±0.48	1.75±0.11	0.945	3.51
	313	10	1.60±0.67	1.01±0.16	0.947	5.02
		20	5.46±0.64	1.45±0.15	0.912	6.32
		30	7.96±0.51	1.58±0.12	0.952	3.97

Table 5. Thermodynamic data of adsorption of Zr-IDA-LG toward catechol and amoxicillin

Adsorbate	E_a/ (kJ·mol^{-1})	ΔH/ (kJ·mol^{-1})	ΔS/ (J·mol^{-1}·K^{-1})	ΔG/(kJ·mol^{-1})		
				293 K	303 K	313 K
Catechol	14.0	24.6	99.8	−5.13	−5.72	−6.64
Amoxicillin	29.9	39.6	149	−3.92	−5.32	−6.90

Constant equation had larger R^2 (>0.90) and smaller SSE, so they could be used to describe the adsorption behavior, indicating the presence of non-homogeneous diffusion in the adsorption process.

2-5. Thermodynamic Parameter Analysis

The adsorption process is generally accompanied with the change of the heat of reaction. Thermodynamic calculations of the adsorption process can yield various parameters, mainly the Gibbs free energy change (ΔG), the enthalpy change (ΔH), the entropy change (ΔS) and the apparent activation energy (E_a). The thermodynamic parameters and apparent activation energy of this study could be calculated by formulas (10)-(13). The rate constants used in the equations were provided by pseudo-second-order kinetics. The results are shown in Table 5.

$$K_c=C_{ad,e}/C_e \quad (10)$$

$$\Delta G=-RT\ln K_c \quad (11)$$

$$\Delta G=\Delta H-T\Delta S \quad (12)$$

$$k=-E_a/RT+\ln A \quad (13)$$

where $C_{ad,e}$ is the concentration of adsorbent on the adsorbent at equilibrium and C_e is the concentration remaining in the solution at equilibrium. The equilibrium constant (K_c) needs to be calculated under ideal conditions where the solution is extremely dilute.

The values of thermodynamic parameters are listed in Table 5. It is observed from Table 5 that ΔG<0, ΔH>0 and ΔS>0 about Zr-IDA-LG adsorption for catechol and amoxicillin. This indicates that it is a spontaneous and entropy-increasing endothermic reaction. Among them, E_a<40.0 kJ·mol^{-1}, ΔH<84.0 kJ·mol^{-1}, indicating the chemical adsorption process accompanied with physical adsorption, and the results are consistent with the conclusion of salinity research. Therefore, combined with the results of pH, it is proved that the adsorption process of Zr-IDA-LG for catechol and amoxicillin includes both chemical and physical adsorption.

2-6. Desorption and Regeneration in Batch Mode

The spent or exhausted adsorbent can be regenerated and re-used for further adsorption cycles and this makes its economic benefits, therefore improving the prospects for practical applications [16,43-46]. For the desorption of organic pollutants, 75% ethanol is generally chosen as the desorption solution. As shown in Fig. 7, the catechol was desorbed and regenerated twice, the desorption efficiencies were 68.9%, 62.5%, and the regeneration rates were 58.4% and 55.0%, respectively. For amoxicillin, the desorption efficiencies were 70.3% and 65.5% and regeneration rates were 65.2% and 61.3%, respectively. The above experimental data indicate the material has recycling ability. The principle of desorption is the competition between the hydrogen bond from ethanol, catechol or amoxicillin and the hydroxyl group on the material. Javad also used

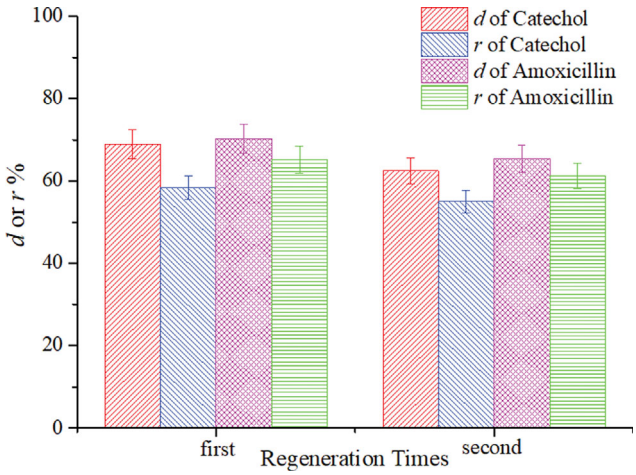

Fig. 7. The results of batch desorption and regeneration.

organic solvents for desorption or regeneration of amoxicillin loaded-adsorbent, and the regeneration efficiency was as high as 97%, and the desorption mechanism was similar to this experiment [42].

3. Fixed-bed Adsorption

3-1. Breakthrough Curve

The results of column adsorption are shown in Fig. 8 and Table 6. To study the influence of column height on adsorption, the concentration of catechol and amoxicillin was controlled at 30 mg·L^{-1}, and the flow rate was 6 mL·min^{-1}. The results are presented in Fig. 8(a_1) and (a_2); the slope of the curve gradually decreases and the half-penetration time increases with the increase in column height. In Table 6, the higher the column height, the higher the removal of catechol and amoxicillin by the adsorbent, the removal of catechol increases from 14.2% to 28.7%, and the removal rate of amoxicillin increases from 17.3% to 43.3%. The reason is that the activation sites on the material are determined by the height of the fixed bed [47]. To explore the effect of concentration, the height of the fixed-bed column was controlled at 5 cm, and the velocity of adsorbate was 6 mL·min^{-1}. Fig. 8(b) shows that as the concentration increases, the penetration slope increases and the half-penetration time decreases (C_0=15 mg·L^{-1}, 30 mg·L^{-1}, 45 mg·L^{-1}), which was with the increase of concentration, the concentration difference between the adsorbent surface and the adsorbent solution is larger and the mass transfer force increases, reaching a short semi-penetration time [48]. It is clearly seen from Fig. 8(c) that the slope of the effluent curve increases and the half-penetration time decreases as the flow rate increases (4 mL·min^{-1}, 6 mL·min^{-1} and 8 mL·min^{-1}). As shown in Table 6, the q_e of Zr-IDA-LG on catechol decreases from 10.7 mg·g^{-1} to 9.33 mg·g^{-1}, the removal rate decreases gradually from 28.3% to 13.3%. The q_e of Zr-IDA-LG on amoxicillin decreases

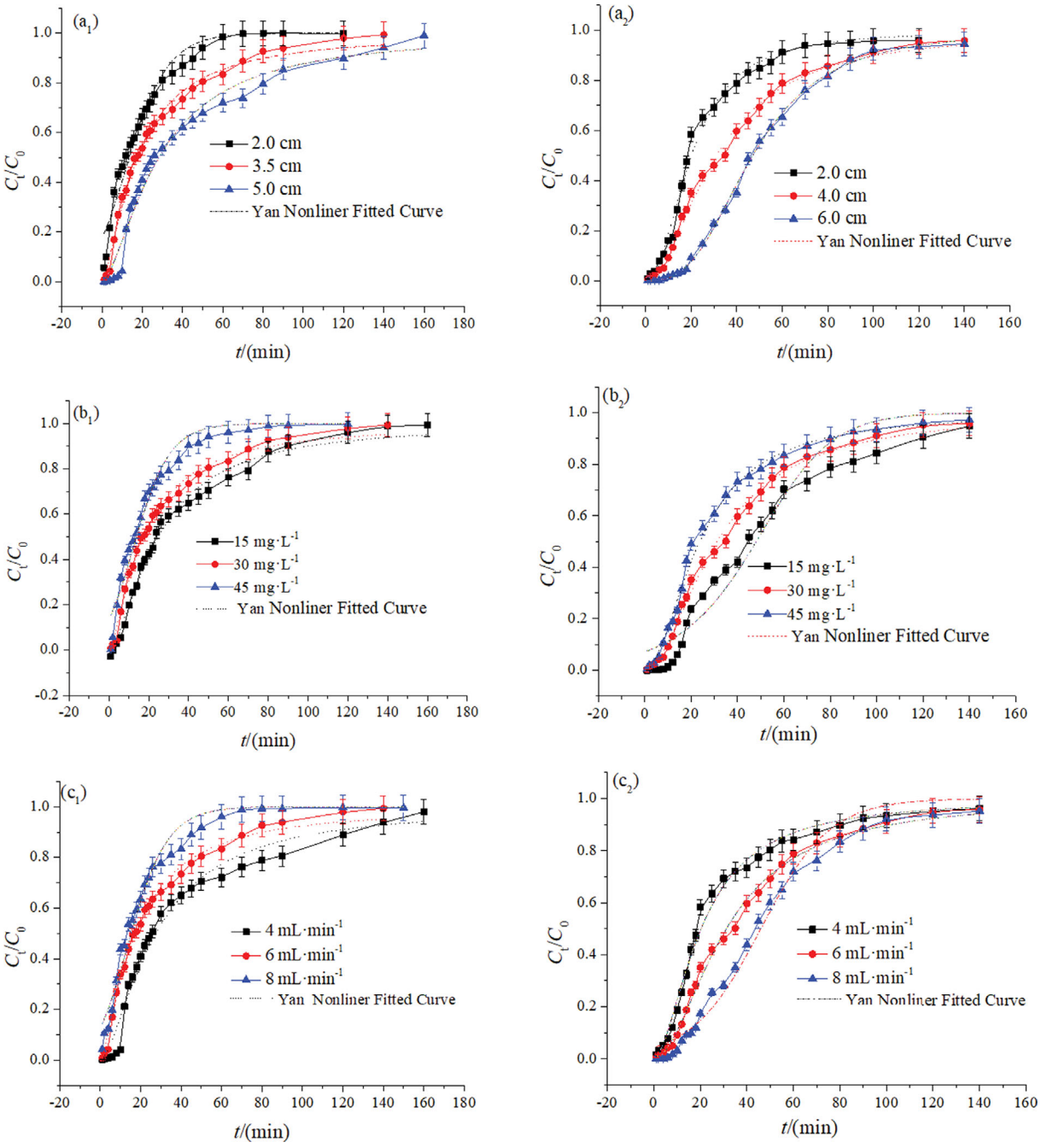

Fig. 8. Effects of different conditions on catechol (subscript 1) and amoxicillin (subscript 2) and Yan model fitting ((a) column height, (b) concentration, (c) flow rate).

from 13.2 mg·g^{-1} to 10.2 mg·g^{-1}, and the removal rate also decreases gradually, from 23.6% to 16.8%. This is the fact that at a slower flow rate, catechol or amoxicillin has enough time to contact with Zr-IDA-LG, so the q_e and the removal rate is higher. To sum up, there is in favor of adsorption with the higher the column and the slower the flow rate. Atefeh et al. achieved the same results in fixed bed adsorption for methylene blue removal with loofah [49].

Compared to adsorption capacity between column mode and batch mode, there is lower about adsorption capacity in column adsorption mode (See Table 4 and 6). Maybe there are two reasons for column adsorption performance with lower adsorption capacity. First, the contact time of adsorbate and adsorbent is lower for column adsorption than that in batch adsorption. Second, the concentration of adsorbate in column adsorption is lower.

3-2. Fixed Bed Model Fitting Analysis

To explore the mechanism of adsorption on catechol and amoxicillin in column mode, we selected the Yan model to describe and analyze the breakthrough curve. The nonlinear fitted curves and fitted parameters are displayed in Fig. 8 and Table 7. From the results of the fixed bed adsorption of catechol and amoxicillin by Zr-

Table 6. Column adsorption data of Zr-IDA-LG toward catechol and amoxicillin

Z/(cm)	v/(mL·min^{-1})	C_0/(mg·L^{-1})	Q_m/(mg)	W_{total}/(mg)	Y/(%)	q_e/(mg·g^{-1})
	Catechol					
2	6	30	3.06	21.6	14.2	9.98
3.5	6	30	5.40	25.2	21.5	10.5
5	6	30	8.25	28.8	28.7	11.4
3.5	6	15	1.71	10.8	15.8	3.33
3.5	6	45	10.3	43.2	23.8	20.0
3.5	4	30	5.52	19.2	28.3	10.7
3.5	8	30	4.80	36.0	13.3	9.33
	Amoxicillin					
2	6	30	3.42	19.8	17.3	11.7
4	6	30	7.74	25.2	30.7	12.9
6	6	30	11.7	27.0	43.3	13.2
4	6	15	4.86	12.6	38.6	8.12
4	6	45	9.45	37.8	25.0	15.8
4	4	30	7.92	23.6	36.4	13.2
4	8	30	6.12	16.8	36.4	10.2

Table 7. The Yan model fitting results for catechol and amoxicillin in fixed bed adsorption

Z/ cm	v/ (mL·min^{-1})	C_0/ (mg·L^{-1})	a	b mL	$q_{e(theo)}$/ (mg·g^{-1})	$q_{e(exp)}$/ (mg·g^{-1})	R^2	SSE×10^{-4}
	Catechol							
2.0	6	30	1.40±0.07	66.2±2.6	8.15	14.6	0.981	3.47
3.5	6	30	1.44±0.05	105±2	7.44	9.85	0.992	1.58
5.0	6	30	1.55±0.09	170±6	8.33	7.23	0.977	5.65
3.5	6	15	3.62±0.18	148±3	5.14	7.46	0.990	2.47
3.5	6	45	1.54±0.06	70.0±1.9	9.41	13.5	0.990	2.01
3.5	4	30	1.57±0.09	110±4	7.40	7.76	0.977	5.70
3.5	8	30	1.63±0.06	106±3	7.28	11.0	0.991	1.98
	Amoxicillin							
2.0	6	30	2.13±0.09	121±3	14.9	19.2	0.992	9.75
4.0	6	30	1.85±0.05	187±3	12.8	13.1	0.996	4.78
6.0	6	30	1.55±0.09	282±2	10.9	11.2	0.999	1.77
4.0	6	15	1.62±0.08	248±3	7.23	8.24	0.994	6.47
4.0	6	45	1.85±0.05	142±2	12.7	13.5	0.995	5.96
4.0	4	30	1.74±0.07	192±2	9.36	7.76	0.992	5.70
4.0	8	30	1.74±0.07	162±4	9.66	11.8	0.991	9.71

IDA-LG, the Yan model had a high R^2 (>0.97) and a small SSE. In Fig. 8, the fitting curves of Yan model and the experimental curves have a higher consistency, so the Yan model could preferably reflect the column adsorption by Zr-IDA-LG on catechol and amoxicillin.

3-3. Fixed Bed Desorption and Regeneration

The column heights of Zr-IDA-LG were 3.5 cm and 4.0 cm, the concentration of catechol and amoxicillin was 30 mg·L^{-1}, and the flow rate was 6 mL·min^{-1}, respectively. After the adsorption, 75% ethanol was selected for desorption. By integrating the curve, the desorption and regeneration was repeated twice, and the curves are shown in Fig. 9. The first unit adsorption capacity of Zr-IDA-LG was 10.5 mg·g^{-1}, the efficiencies of desorption were 86.6%, 60.9%, and the regeneration rates were 80.0%, 62.5%, respectively. Compared with the static desorption and regeneration, the desorption and regeneration rates were improved. The first unit adsorption capacity of amoxicillin adsorption by Zr-IDA-LG was 12.9 mg·g^{-1}, the desorption rates were 67.0%, 44.7%, and the regeneration rates were 71.2%, 49.0%, respectively. Both desorptions were basically completed within 30 min, with fast rate and high desorption rate, indicating that Zr-IDA-LG could be reused.

4. XPS and Mechanism Analysis

To explore the adsorption mechanism of Zr-IDA-LG on catechol and amoxicillin, elemental content and element peak spectra before and after adsorption of Zr-IDA-LG were investigated by XPS. In the XPS full spectrum of adsorbed catechol (Fig. 10), the contents of C, O, N, and Zr elements in Zr-IDA-LG were 62.1%, 34.8%,

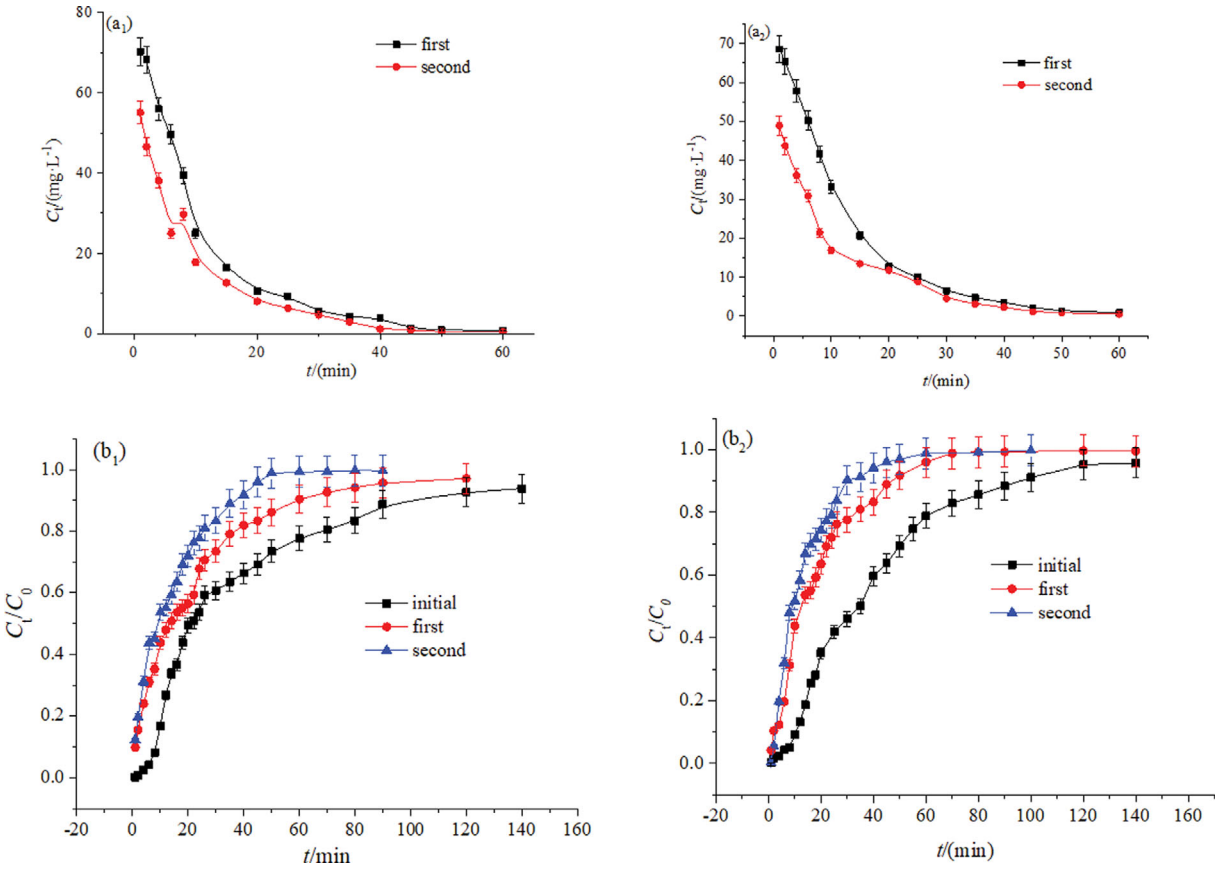

Fig. 9. The results of fixed bed desorption and regeneration ((a) desorption; (b) regeneration).

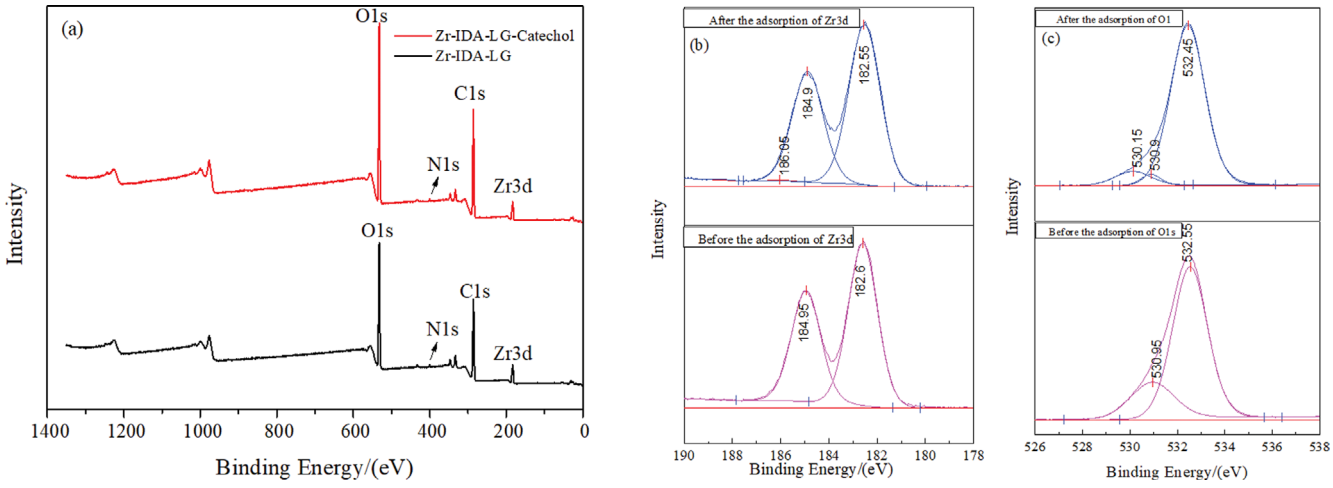

Fig. 10. (a) Full XPS spectrum of adsorption of catechol; (b) Zr3d and (c) O1s spectrum.

1.74%, and 1.35%, respectively. After the adsorption, the contents of C, O, N and Zr were 45.0%, 51.9%, 1.20% and 1.89%, respectively, and the oxygen element content increased significantly, which demonstrated that the catechol migrated successfully to the adsorbent during the adsorption process. Before the adsorption of catechol, Zr3d appeared Zr-O bond peaks, which was the complexation between zirconium chloride and the carboxyl group on iminodiacetic acid in the preparation stage. After the adsorption, Zr3d was separated into three peaks at 182.55 eV, 185.38 eV and 186.05 eV. Similarly, O1s was divided into three peaks at 532.45 eV, 530.9 eV, and 530.15 eV, and the peak area percentages were 87.8%, 3.69%, and 8.46%, indicating that the zirconium on Zr-IDA-LG was related to the hydroxyl oxygen in catechol [50]. By analyzing the adsorption properties of zirconium and the molecular structure of catechol, it was found that zirconium complexed with the ortho-dihydroxyl group to obtain structurally stable five-membered rings. Also there

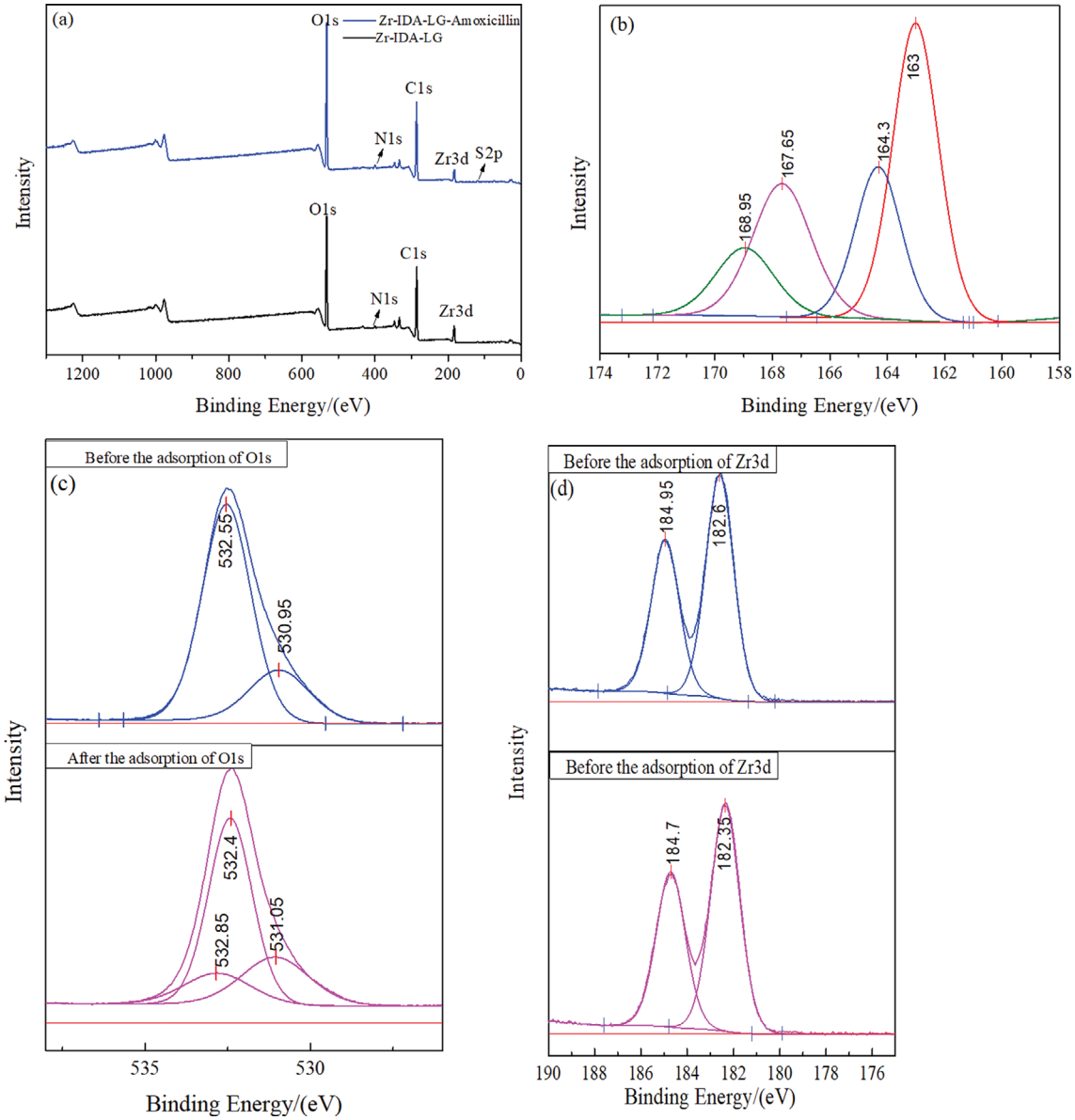

Fig. 11. (a) Full XPS spectrum of adsorption of amoxicillin; (b) S2p and (c) O1s and (d) Zr3d spectrum.

was electrostatic attraction from the effect of salts on adsorption.

Fig. 11 is the XPS analysis of Zr-IDA-LG for amoxicillin. The content of C, O, N, Zr and S elements contained in Zr-IDA-LG after adsorption of amoxicillin was 38.2%, 58.8%, 1.20%, 1.35% and 0.410%, respectively, and the content of O and S elements increased significantly after adsorption (it was known from the molecular structure of amoxicillin that each molecule contains one sulfur atom), which certified that the adsorbent successfully adsorbed amoxicillin. After the adsorption of amoxicillin, Zr3d was separated into two peaks at 182.35 eV and 184.7 eV, and O1s was separated into three peaks at 532.45 eV, 530.9 eV and 530.15 eV, which were generated by the combination of zirconium on the material and the carboxyl oxygen in the amoxicillin molecule. And S2p peaks obviously appeared at 168.95 eV, 167.65 eV, 164.3 eV, and 163 eV, which were the energy spectrum peaks of sulfur in the amoxicillin adsorbed on the Zr-IDA-LG. By analyzing the isoelectric point of the material and the molecular structure of amoxicillin, at pH<7.49, the amoxicillin molecule had a protonated amino group, the negatively charged functional group on Zr-IDA-LG (ionized carboxyl group) and amoxicillin molecule directly generated electrostatic attraction. In addition, there may also exist ion exchange during the adsorption process, mainly from the ion exchange of the protonated hydroxyl group on the material and the protonated group on amoxicillin.

Fig. 12 shows the speculated mechanism of catechol and Amoxicillin onto Zr-IDA-LG.

CONCLUSION

One new biocomposite, zirconium-modified (Zr-IDA-LG) was prepared and used as adsorbent. The adsorption properties of Zr-IDA-LG toward catechol and amoxicillin were investigated in batch mode and column (fixed-bed) mode. The adsorption per-

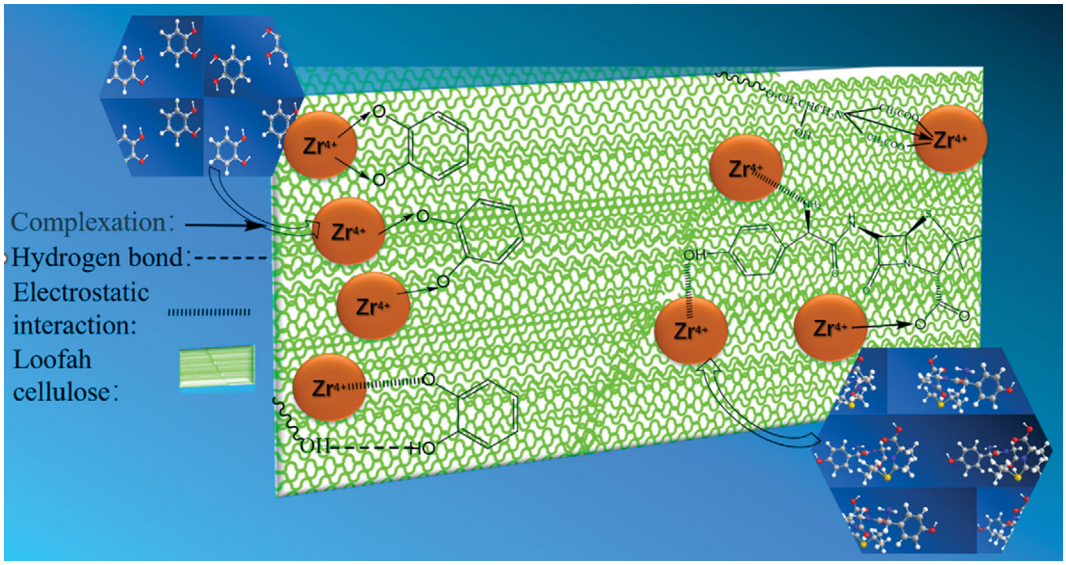

Fig. 12. The mechanism diagram of adsorption on catechol and amoxicillin.

formance of Zr-IDA-LG for catechol and amoxicillin was significantly improved after modification. The adsorption of catechol was monolayer complex with diffusion process. Similarly, the adsorption of amoxicillin was a hybrid chemisorption process accompanied by heterogeneous diffusion. In fixed bed adsorption, the adsorption was consistent with the Yan model. There is good property of regeneration for spent Zr-IDA-LG. The main mechanism of adsorption is complexation and electrostatic attraction for catechol and amoxicillin. In conclusion, Zr-IDA-LG is not only green and simple in synthesis process, but also easy to separate and recycle. Therefore, it is a promising adsorbent for removing organic pollutants.

ACKNOWLEDGEMENTS

This work was financially supported by the Henan province basis and advancing technology research project (142300410224).

REFERENCES

1. H. Ma, X. Zhang, Q. Ma and B. Wang, *J. Hazard. Mater.*, **165**, 475 (2009).
2. R. R. Karri, N. S. Jayakumar and J. N. Sahu, *J. Mol. Liq.*, **231**, 249 (2017).
3. C. Zhang, X. Wang, Z. Ma, Z. Luan, Y. Wang, Z. Wang and L. Wang, *Environ. Chem. Lett.*, **18**, 377 (2020).
4. Y. H. Fu, Y. F. Shen, Z. D. Zhang, X. L. Ge and M. D. Chen, *Sci. Total Environ.*, **646**, 1567 (2019).
5. D. Y. Ma, S. Y. Zhang, S. H. Zhan, L. T. Feng, S. G. Zeng, Q. Q. Lin and Y. Pan, *Ind. Eng. Chem. Res.*, **58**, 20090 (2019).
6. N. Schweigert, A. J. B. Zehnder and R. I. L. Eggen, *Environ. Microbiol.*, **3**, 81 (2001).
7. B. F. Negara, J. H. Sohn, J. S. Kim and J. S. Choi, *Foods*, **10**, 452 (2021).
8. B. A. de Marco, J. S. H. Natori, S. Fanelli, E. G. Tótoli and H. R. N. Salgado, *Crit. Rev. Anal. Chem.*, **47**, 267 (2017).
9. L. W. Matzek and K. E. Carter, *Chemosphere*, **151**, 178 (2016).
10. W. R. Chen, Y. J. Ding, C. T. Johnston, B. J. Teppen, S. A. Boyd and H. Li, *Environ. Sci. Technol.*, **44**, 4486 (2010).
11. K. Kummerer, *Chemosphere*, **75**, 435 (2009).
12. A. A. Aryee, R. P. Han and L. B. Qu, *J. Clean. Prod.*, **368**, 133140 (2022).
13. A. Hrioua, A. Loudiki, A. Farahi, F. Laghrib, M. Bakasse, S. Lahrich, S. Saqrane and M. A. El Mhammedi, *Bioelectrochemistry*, **142**, 107936 (2021).
14. F. M. Mpatani, R. P. Han, A. A. Aryee, A. N. Kani, L. B. Qu and Z. H. Li, *Sci. Total Environ.*, **780**, 146629 (2021).
15. F. Zhu, Y. M. Zheng, B. G. Zhang and Y. R. Dai, *J. Hazard. Mater.*, **401**, 123608 (2021).
16. J. L. Wang, X. Liu, M. M. Yang, H. Y. Han, S. S. Zhang, G. F. Ouyang and R. P. Han, *J. Mol. Liq.*, **338**, 116698 (2021).
17. X. Xu, B. Y. Gao, B. Jin and Q. Y. Yue, *J. Mol. Liq.*, **215**, 565 (2016).
18. S. Su, Q. Liu, J. Liu, H. Zhang, R. Li, X. Jing and J. Wang, *J. Colloid Interface Sci.*, **530**, 538 (2018).
19. D. K. Verma, S. H. Hasan, D. Ranjan and R. M. Banik, *Int. J. Environ. Sci. Technol.*, **11**, 1927 (2014).
20. I. Anastopoulos and I. Pashalidis, *J. Mol. Liq.*, **319**, 114127 (2020).
21. R. Ahmad and S. Haseeb, *Desal. Water Treat.*, **57**, 17826 (2016).
22. Q. Kong, Y. N. Wang, L. Shu and M. S. Miao, *Desalin. Water Treat.*, **57**, 7933 (2016).
23. R. Tyagi and J. Jacob, *React. Funct. Polym.*, **154**, 104687 (2020).
24. A. A. Aryee, F. M. Mpatani, Y. Y. Du, A. N. Kani, E. Dovi, R. P. Han, Z. H. Li and L. B. Qu, *Environ. Pollut.*, **268**, 115729 (2021).
25. P. A. Kavaklı, C. Kavaklı and O. Güven, *Rad. Phys. Chem.*, **94**, 105 (2014).
26. M. Y. Liu, X. T. Zhang, Z. H. Li, L. B. Qu and R. P. Han, *Carbohyd. Polym.*, **248**, 116792 (2020).
27. K. K. Zhu, Y. F. Gu, R. Wang and R. P. Han, *Desal. Water Treat.*, **236**, 274 (2021).
28. B. R. Poudel, R. L. Aryal, S. K. Gautam, K. N. Ghimire, H. Paudyal and M. R. Pokhrel, *J. Environ. Chem. Eng.*, **9**, 106552 (2021).

29. J. L. Wang, X. Liu, H. Y. Han and R. P. Han, *Desal. Water Treat.*, **253**, 256 (2022).
30. D. Z. Marković-Nikolić, A. L. Bojić, S. R. Savić, S. M. Petrović, D. J. Cvetković, M. D. Cakić and G. S. Nikolić, *J. Spectrosc.*, **2018**, 1856109 (2018).
31. G. Yuvaraja, Y. X. Pang, D. Y. Chen, L. J. Kong, S. Mehmood, M. V. Subbaiah, D. S. Rao, C. M. Pavuluri, J. C. Wen and G. M. Reddy, *Int. J. Biol. Macromol.*, **136**, 177 (2019).
32. M. A. Aslam, W. Ding, S. U. Rehman, A. Hassan, Y. C. Bian, Q. C. Liu and Z. G. Sheng, *Appl. Surf. Sci.*, **543**, 148785 (2021).
33. A. Naskar and R. Majumder, *J. Mol. Liq.*, **242**, 892 (2017).
34. X. C. Jin, Z. Y. Xiang, Q. G. Liu, Y. Chen and F. C. Lu, *Bioresour. Technol.*, **244**, 844 (2017).
35. A. Ogawa and H. Fujimoto, *Inorg. Chem.*, **41**, 4888 (2002).
36. K. Shakir, H. F. Ghoneimy, A. F. Elkafrawy, S. G. Beheir and M. Refaat, *J. Hazard. Mater.*, **150**, 765 (2008).
37. S. Miyata, *Clay. Clay Miner.*, **31**, 305 (1983).
38. K. V. Kumar, S. Gadipelli, B. Wood, K. A. Ramisetty, A. A. Stewart, C. A. Howard, D. J. L. Brett and F. Rodriguez-Reinoso, *J. Mater. Chem. A*, **7**, 10104 (2019).
39. H. Niknejad, A. Esrafili, M. Kermani, V. Oskoei and M. Farzadkia, *J. Environ. Health Sci. Eng.*, **18**, 1521 (2020).
40. M. Khajavian, S. Shahsavarifar, E. Salehi, V. Vatanpour, M. Masteri-Farahani, F. Ghaffari and S. A. Tabatabaei, *Chem. Eng. Res. Des.*, **175**, 131 (2021).
41. E. Vunain, D. Houndedjihou, M. Monjerezi, A. A. Muleja and B. Kodom, *Water Air Soil Pollut.*, **229**, 366 (2018).
42. J. Imanipoor, M. Mohammadi, M. Dinari and M. R. Ehsani, *J. Chem. Eng. Data*, **66**, 389 (2021).
43. C. H. Ma, X. T. Zhang, K. Wen, R. Wang and R. P. Han, *Korean J. Chem. Eng.*, **38**(1), 135 (2021).
44. X. T. Zhang, S. S. Zhang, G. F. Ouyang and R. P. Han, *Korean J. Chem. Eng.*, **39**(7), 1839 (2022).
45. Y. N. Shang, X. Xu, Q. Y. Yue, B. Y. Gao and Y. W. Li, *Environ. Sci. Nano*, **7**, 1444 (2020).
46. A. A. Aryee, E. Dovi, R. P. Han, Z. H. Li and L. B. Qu, *J. Colloid Interface Sci.*, **598**, 69 (2021).
47. Z. Akzu and F. Gonen, *Process Biochem.*, **39**, 599 (2004).
48. E. Dovi, A. A. Aryee, A. N. Kani, F. M. Mpatani, J. J. Li, L. B. Qu and R. P. Han, *J. Environ. Chem. Eng.*, **10**(2), 107292 (2022).
49. A. Baharlouei, E. Jalilnejad and M. Sirousazar, *Chem. Eng. Commun.*, **205**, 1537 (2018).
50. B. Debnath, M. Majumdar, M. Bhowmik, K. L. Bhowmik, A. Debnath and D. N. Roy, *J. Environ. Manage.*, **261**, 110235 (2020).